α-decay, two-proton emission and cluster decay half-lives

XIV. International Conference on Nuclear Structure Properties (Selcuk University, Konya, Turkey).

Harjeet Kaur

Department of Physics, Guru Nanak Dev University, Amritsar, Punjab-143005.

June 3, 2021

Proximity potentials

- Proximity potentials have been proved to be very effective in the calculations of half-lives of heavy and superheavy nuclei since their development by Blocki in 1977.
- Nagib predicted half-lives of unknown SHN with $Z = 122-125$ using theoretical model consisting of proximity potential after testing the model for forty known SHN.
- Convenient empirical relations connecting half-lives and Q_α-values are also being employed now-a-days [Deng *et al.*(2020)Deng, Zhang, and Royer, Akrawy and Ahmed(2019), Poenaru and Gherghescu(2018)].

α-decay half-life

α-decay can be explained as the penetration of the already formed α- particle through the interaction potential barrier $V(r,\theta)$

$$V(r,\theta) = V_C(r,\theta) + V_P(r,\theta) \tag{1}$$

where

$$V_C(r,\theta) = 2Z_D e^2 \begin{cases} 1/r & \text{for} \quad r \geq r_c \\ \frac{1}{2r_c}\left(3 - \left(\frac{r}{r_c}\right)^2\right) & \text{for} \quad r < r_c \end{cases}. \tag{2}$$

Here, $r_c = r_\alpha + r_d$ and, the nuclear radius r_i in general can be found using the following formula:

$$r_i = \{1.28A_i^{1/3} - 0.76 + 0.8A_i^{-1/3}\} \times (1 + \beta_2 Y_{20}(\theta) + \beta_4 Y_{40}(\theta)) \tag{3}$$

where $i = \alpha, d, p$ representing the radii of an $\alpha-$ particle, daughter and parent nuclei.

For a two-body shape, an analytical formalism for proximity potential is described as [Royer(2010)]:

$$
\begin{aligned}
V_P(r,\theta) &= 4\pi\gamma e^{-1.38(r-r_\alpha-r_d)}\left[0.6584A^{2/3}-\left(\frac{0.172}{A^{1/3}}\right.\right. \\
&+ \left.\left. 0.4692A^{1/3}\right) r - 0.02548A^{1/3}r^2+0.01762\ r^3\right]
\end{aligned} \tag{4}
$$

$$
\text{where} \quad \gamma = 0.9517\sqrt{1-2.6\left(\frac{A_d-2Z_d}{A_d}\right)^2}. \tag{5}
$$

Penetration probability K can be evaluated as:

$$
K = \int_0^{\pi/2} d\theta \frac{\sin\theta}{1+\exp\left(q(\theta)\right)} \tag{6}
$$

where

$$
q(\theta) = \exp\left[\frac{2}{\hbar}\int_{a'(\theta)}^{b'(\theta)}\sqrt{2\mu(V(r,\theta)-Q_\alpha)}\ \ dr\right] \tag{7}
$$

with $\mu = 0.98M_\alpha$, turning point $b'(\theta)$ is fixed such that $V(b'(\theta)) = Q_\alpha$ while the turning point $a'(\theta)$ is taken as r_c.

Using equation (7), $T_{1/2}^{\alpha,th}(s)$ can be found as,

$$T_{1/2}^{\alpha,th}(s) = \frac{\ln 2}{K v_0 P_0}. \tag{8}$$

v_0 is the assault frequency which is given as

$$v_0 = \frac{1}{2r_p}\sqrt{\frac{2E_\alpha}{M_\alpha}} \tag{9}$$

and E_α is the kinetic energy of $\alpha-$ particle [Budaca *et al.*(2016)Budaca, Budaca, and Silisteanu]:

$$E_\alpha = \left[Q_\alpha - \left(6.53 Z_d^{7/5} - 8.0 Z_d^{2/5}\right) 10^{-5}\right] \frac{A_d}{A_p} \ \ \mathrm{MeV}.$$

We have used the preformation probability P_0 [Zhang *et al.*(2009)Zhang, Royer, Wang, Dong, Zuo, and Li]

$$\begin{aligned} \log_{10} P_0 &= (34.90593 + 0.003011(Z-82)(126-Z) \\ &+ 0.003717(N-152)(184-N) - 0.151216A \\ &+ 0.006681(Z-82)(N-152)). \end{aligned} \tag{10}$$

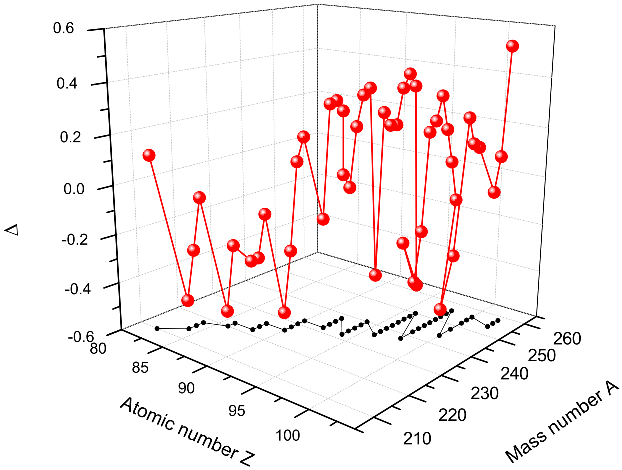

Figure 1: The differences (Δ) between the experimental logarithmic values of half-lives [Cui *et al.*(2018)Cui, Zhang, Zhang, and Wang] and the theoretical ones obtained using expression (17) for even-even with $Z = 82 - 102$ are plotted. Maximum value of $|\Delta|$ is obtained as 0.527.

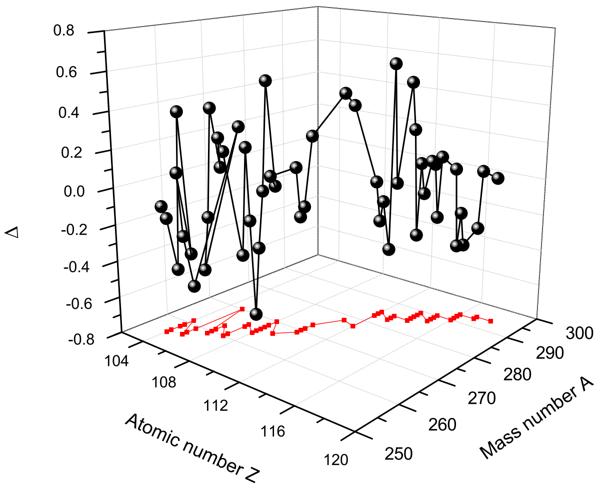

Figure 2: Differences (Δ) between the experimental logarithmic values of half-lives [Cui *et al.*(2018)Cui, Zhang, Zhang, and Wang] and the theoretical ones obtained using expression (17) for SHN with $Z = 104 - 118$ are described and maximum value obtained is 0.613.

Comparison with other models

Model	nuclei	$\sqrt{\bar{\delta}^2}$	$\lvert\bar{\delta}\rvert$	$\bar{\delta}$	$\lvert\Delta_{max}\rvert$
Theor-	e-e	0.279	0.242	-0.014	0.527
-etical	SHN	0.291	0.236	-0.030	0.705
MVS	e-e	0.281	0.235	-0.087	0.790
	SHN	0.681	0.548	-0.138	1.653
Royer's	e-e	0.311	-0.103	0.264	0.911
	SHN	0.481	0.398	0.090	1.128
VS	e-e	0.314	0.209	-0.032	1.459
	SHN	0.612	0.502	-0.289	1.144
Brown	e-e	0.334	0.278	-0.003	0.709
	SHN	0.763	0.637	0.625	1.464
UNIV	e-e	0.359	0.300	0.063	0.810
	SHN	-	-	-	-
AKRA	e-e	0.412	0.291	-0.204	1.511
	SHN	0.723	0.613	-0.456	1.374

modified	e-e	0.414	0.355	-0.227	1.143
Royer's	SHN	0.476	0.387	0.027	1.421
mB1	e-e	0.646	0.440	-0.335	1.752
	SHN	0.311	0.241	0.024	1.131
mB2	e-e	1.292	-0.985	1.063	2.846
	SHN	0.324	0.243	0.021	0.993
MMF	e-e	1.300	1.064	0.473	2.602
	SHN	1.469	1.300	1.299	3.370

Root-mean-square value: $\sqrt{\bar{\delta^2}} = \sqrt{\frac{1}{N'} \sum_1^{N'} \Delta_i^2}$
Mean deviation: $|\bar{\delta}| = \frac{1}{N'} \sum_1^{N'} |\Delta_i|$
Mean of errors $\bar{\delta} = \frac{1}{N'} \sum_1^{N'} \Delta_i$ where
$\Delta_i = \log_{10}[T_{1/2}^{\alpha,exp}(s)] - \log_{10}[T_{1/2}^{\alpha,th}(s)]$ and N' are the maximum number of nuclei we considered for our study.

Two-proton radioactivity

- Two-proton radioactivity of nuclei was predicted by Zel'dovich and Goldansky in the 1960s.
- However, experimentally it was first observed in ^{45}Fe at GSI and at GANIL in 2002, respectively.
- Then, it was discovered in ^{54}Zn, ^{48}Ni, ^{19}Mg, and ^{67}Kr.
- Also, very short-lived ground-state two-proton radioactivity was observed in ^{6}Be, ^{12}O and ^{16}Ne.
- Theoretical methods describing such radioactivity involve Direct decay model, simultaneous versus sequential decay model, diproton model and three-body models.
- Recently, Gonçalves et al. calculated the half-lives of the 2p radioactive nuclei using ELDM while Cui et al. exploited GLDM for the same.

Theory

Again, we have considered that two-proton decay can be explained as the penetration of the two protons through the interaction potential barrier $V(r,\theta)$ comprising of the Coulomb potential $V_C(r,\theta)$ and the proximity potential $V_P(r,\theta)$ i.e.

$$V(r,\theta) = V_C(r,\theta) + V_P(r,\theta) \tag{11}$$

$V_C(r,\theta)$ is Coulomb potential (eq. (2)) while $V_P(r,\theta)$ takes the form as described in eq. (4) with

$$\text{where} \quad \gamma = 0.9517\sqrt{1 - 1.7826\left(\frac{A_d - 2Z_d}{A_d}\right)^2}. \tag{12}$$

In this case, protons are considered as point charges. So, we have chosen $r_{2p} = 0$. Now, after find the penetration probability K, we can find $T_{1/2}^{2p,th}(s)$ can be found as,

$$T_{1/2}^{2p,th}(s) = \frac{\ln 2}{K v_0}. \tag{13}$$

Here, v_0 is the assault frequency and it is given as

$$v_0 = \frac{1}{2R_p}\sqrt{\frac{2E_{2p}}{M_{2p}}} \tag{14}$$

where M_{2p} is the mass of two protons and E_{2p} is the kinetic energy of protons while R_p is the radius of parent nucleus.

Results and discussion

Nucleus	Q_{2p}	$\log_{10}[T_{1/2}^{2p}(s)]$				
		GLDM	ELDM	Exp.	Our	Δ
^{12}O	1.638	-19.17	-18.27	>-19.40	-19.062	-0.154
		1.820	-19.46	-20.14	-19.345	-0.614
		1.790	-19.43	-20.31	-19.301	-0.826
		1.800	-19.44	-20.32	-19.317	-0.821
^{16}Ne	1.330	-16.45		-19.84	-17.052	-2.553
	1.400	-16.63	-16.60	-19.58	-17.259	-2.086
^{19}Mg	0.750	-11.79	-11.72	-11.40	-12.174	1.053
^{45}Fe	1.100	-2.23		-2.40	-2.153	0.260
	1.140	-2.71		-2.07	-2.640	0.993
	1.154	-2.87	-2.43	-2.55	-2.805	0.761
	1.210	-3.50		-2.42	-3.434	1.519
^{48}Ni	1.290	-2.62		-2.52	-2.587	0.454
	1.350	-3.24		-2.08	-3.200	1.656
	1.310	-2.83	-2.36	-2.52	-2.798	0.663

Nucleus	Q_{2p}			$\log_{10}[T_{1/2}^{2p}(s)]$		
		GLDM	ELDM	Exp.	Our	Δ
^{54}Zn	1.280	-0.87		-2.76	-0.847	-1.346
	1.480	-2.95	-2.52	-2.43	-2.940	1.072
^{67}Kr	1.690	-1.25	-0.06	-1.70	-0.735	-0.502

The maximum value of Δ obtained for the two-proton emission half-lives determined using GLDM model is -3.40 [Cui *et al.*(2020)Cui, Gao, Wang, and Gu] while in our case this value is obtained as -2.553.

Cluster-decay

Cluster-decay half-lives can be found after finding penetration probability of cluster through interaction potential barrier involving Coulomb potential $V_C(r,\theta)$ and proximity potential $V_P(r,\theta)$. Analytical formalism for proximity potential in this case is described as [Royer(2010)]:

$$\begin{aligned} V_P(r,\theta) &= 4\pi\gamma\frac{C_1C_2}{C1+C2} \\ &\times \left[\frac{-0.0527}{0.025e^{0.12(r-C_1-C_2)}+0.0085e^{1.52(r-C_1-C_2)}}\right. \\ &+ \left.\frac{1.956}{r^2}-\frac{0.142}{r}\right] \end{aligned} \tag{15}$$

$$\begin{aligned} \text{where } \gamma &= 0.9517\sqrt{1-2.6\left(\frac{A_d-2Z_d}{A_d}\right)^2} \\ &\times \sqrt{1-2.6\left(\frac{A_{cl}-2Z_{cl}}{A_{cl}}\right)^2} \end{aligned} \tag{16}$$

and $C_i = R_i - \frac{b^2}{2R_i}$ with b as surface width chosen to be 1 fm. R_i represents nuclear radius.
Half-life $T_{1/2}^{cl,th}(s)$ can be found as,

$$T_{1/2}^{cl,th}(s) = \frac{\ln 2}{K v_0 P_0}. \tag{17}$$

K is the penetration probability, v_0 is the assault frequency:

$$v_0 = \frac{1}{2R_P}\sqrt{\frac{2E_v}{M_c}\left(1 - \frac{M_c}{M_p}\right)} \tag{18}$$

M_c is mass of cluster while M_p is the mass of parent nucleus.
E_v is the vibrational energy and it is given as:

$$E_v = Q_c\left(0.056 + 0.039\exp\left(\frac{4 - A_{cl}}{2.5}\right)\right) \tag{19}$$

We have used the following form of the preformation probability P_0

$$P_0 = \begin{array}{c} -\frac{1.481}{Z_{cl}}\sqrt{Z_d Z_{cl}\mu} + 29.3158 I_{cl} - 1.25385 \quad \text{for} \quad Z_{cl} > 10 \\ -\frac{0.047 A_{cl}}{Z_{cl}}\sqrt{Z_d Z_{cl}\mu} + 29.3158 I_{cl} - 1.25385 \quad \text{for} \quad Z_{cl} \leq 10 \end{array}$$

where $I_{cl} = \frac{N_{cl} - Z_{cl}}{A_{cl}}$

Results and discussion

Parent Nucleus	Cluster	$Q_c^{Exp.}$	$\log_{10}[T_{1/2}^{cl}(s)]$	
			Theor.	Exp.
		(MeV)		
^{222}Ra	^{14}C	33.05	11.97	11.22
^{224}Ra	^{14}C	30.54	16.59	15.86
^{226}Ra	^{14}C	28.21	21.51	21.34
^{228}Th	^{20}O	44.72	21.24	20.72
^{230}Th	^{24}Ne	57.78	24.63	24.61
^{232}Th	^{24}Ne	55.62	29.43	$>$ 29.20
^{230}U	^{22}Ne	61.40	18.92	19.57
^{232}U	^{24}Ne	62.31	20.69	21.08
^{232}U	^{28}Mg	74.32	25.29	$>$22.26
^{234}U	^{24}Ne	58.84	25.57	25.92
^{234}U	^{26}Ne	59.47	24.83	25.92
^{234}U	^{28}Mg	74.13	25.40	25.14

Parent Nucleus	Cluster	$Q_c^{Exp.}$	$\log_{10}[T_{1/2}^{cl}(s)]$	
			Theor.	Exp.
		(MeV)		
^{236}U	^{24}Ne	55.96	28.50	$>$25.90
^{236}U	^{26}Ne	56.75	28.04	$>$25.90
^{236}U	^{28}Mg	1.69	28.51	27.58
^{236}U	^{30}Mg	72.51	28.35	27.58
^{236}Pu	^{28}Mg	79.67	21.39	21.67
^{238}Pu	^{28}Mg	75.93	25.83	25.70
^{238}Pu	^{30}Mg	77.03	25.33	25.70
^{238}Pu	^{32}Si	91.21	25.45	25.27
^{240}Pu	^{34}Si	90.95	25.53	$>$ 25.52
^{242}Cm	^{34}Si	96.53	22.31	23.15

Conclusion

- We have determined α-decay half-lives ($T^{\alpha}_{1/2}$-values) of superheavy nuclei (SHN) employing the interaction potential involving Coulomb and proximity potential.
- We juxtapose our results for half-lives with the experimental ones and the r.m.s. value is obtained as 0.291 which is the lowest.
- Thus the accuracy of this model has been tested and a comparison has been drawn with the other empirical and theoretical methods.
- Also, we determine the two-proton emission half-lives and cluster-decay half-lives.
- Agreement of our results with the experimental ones is fair enough.

- J.-G. Deng, H.-F. Zhang, and G. Royer, Phys. Rev. C **101**, 034307 (2020).
- D. T. Akrawy and A. H. Ahmed, Phys. Rev. C **100**, 044618 (2019).
- D. N. Poenaru and R. Gherghescu, Physical Review C **97**, 044621 (2018).
- G. Royer, Nuclear Physics A **848**, 279 (2010).
- A. Budaca, R. Budaca, and I. Silisteanu, Nuclear Physics A **951**, 60–74 (2016).
- H. F. Zhang, G. Royer, Y. J. Wang, J. M. Dong, W. Zuo, and J. Q. Li, Phys. Rev. C **80**, 057301 (2009).
- J. P. Cui, Y. L. Zhang, S. Zhang, and Y. Z. Wang, Physical Review C **97**, 014316 (2018).
- J. P. Cui, Y. H. Gao, Y. Z. Wang, and J. Z. Gu, Phys. Rev. C **101**, 014301 (2020).